

# Environment-Assisted Quantum Transport

Patrick Rebentrost,<sup>1</sup> Masoud Mohseni,<sup>1</sup> Ivan Kassal,<sup>1</sup> Seth Lloyd,<sup>2</sup> and Alán Aspuru-Guzik<sup>1</sup>

<sup>1</sup>*Department of Chemistry and Chemical Biology, Harvard University, 12 Oxford St., Cambridge, MA 02138*

<sup>2</sup>*Department of Mechanical Engineering, Massachusetts Institute of Technology, 77 Massachusetts Avenue, Cambridge MA 02139*

(Dated: May 27, 2022)

Transport phenomena at the nano-scale are of interest due to the presence of both quantum and classical behavior. In this work, we demonstrate that quantum transport efficiency can be enhanced by a dynamical interplay of the system Hamiltonian with the pure dephasing dynamics induced by a fluctuating environment. This is in contrast to fully coherent hopping that leads to localization in disordered systems, and to highly incoherent transfer that is eventually suppressed by the quantum Zeno effect. We study these phenomena in the Fenna-Matthews-Olson protein complex as a prototype for larger photosynthetic energy transfer systems. We also show that disordered binary tree structures exhibit enhanced transport in the presence of dephasing.

PACS numbers: 03.65.Yz, 05.60.Gg, 71.35.-y, 03.67.-a

The efficiency of transport in an open quantum system can be substantially affected by the interaction with a fluctuating environment. Noise and decoherence collapse the state generated by quantum hopping and so typically one expects an inhibitory effect on quantum transport. One of the most important classes of quantum transport is the energy transfer in molecular systems [1], for example in the chromophoric light-harvesting complexes [2, 3]. The role of the environment in chromophoric systems [4, 5, 6] and model geometries [7] has been widely studied. The Haken-Strobl model is widely used to describe Markovian bath fluctuations [8]. Gaab and Bardeen used this approach to explore the effect of geometry and coherence in the energy trapping of some model light-harvesting systems [7]. Leegwater [9] uses the survival time to discuss the crossover from hopping to exciton dynamics in the LH1 photosynthetic system of purple bacteria. Quantum transport can also be affected by the well-known Anderson localization [10, 11]. Energy mismatches in disordered materials lead to destructive interference of the electronic wavefunction and subsequently to localization of the quantum particle. Specifically, it has been argued that quantum localization can seriously limit computational power and/or quantum walk properties in binary tree structures [12], where an exponential speed-up over a classical random walk can in principle be observed [13]. Generally, the overall effect of environment and static disorder is expected to be negative. However, as we demonstrate here, in a large variety of transport systems and under proper conditions, the interaction with the environment can result in increased quantum transport efficiency.

Decoherence-enhanced transfer has recently been reported for two quantum dots within the Redfield theory [14]. In chromophoric complexes, an environment-assisted quantum walk within the Lindblad model was used to explain the high energy transfer efficiency [15]. This approach was also used to quantify the percentage contributions of quantum coherence and environment-induced relaxation to the overall efficiency [16]. Noise-induced enhancement can also be seen in stochastic resonance [17], where the quantum system is driven to a non-linear regime. The role of pure dephasing in the quantum localization was also raised in [18]. A review of Anderson localization and its exceptions was given by Phillips [19]. In this work, we study the interaction between

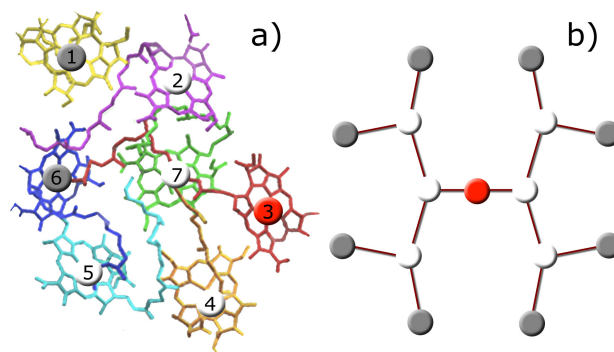


FIG. 1: Quantum transport arises in nature, for example in the energy transfer of photosynthetic complexes and in artificial or engineered systems. In the Fenna-Matthews-Olson protein complex a) quantum coherence has been shown to play a significant role in the exciton dynamics [2]. Binary trees b) are an important concept in many areas of science. Specifically, in quantum physics an exponential speed-up in finding certain target sites (red) make them a potential candidate for the implementation of quantum algorithms [13]. (The grey sites represent initial states for the quantum transport.)

*pure dephasing noise* and coherent dynamics that can result in greatly increased efficiency of transport. Unlike stochastic resonance, this enhancement occurs in undriven systems. The intuition is as follows: In a quantum system with some degree of disorder, localization suppresses transport at low noise levels. By contrast, at very high noise levels, decoherence effectively produces a ‘watchdog effect’ [20] that also suppresses transport. However, at intermediate noise levels coherence and decoherence can collaborate to produce highly efficient transport. This enhancement holds even if the noise itself is purely decohering and can induce no transport on its own. We investigate a general model of such environmentally assisted quantum transport (ENAQT) and apply that model to chromophoric light-harvesting systems, where we show that the interplay between coherence and decoherence leads to maximally efficient transport at a noise level corresponding to ambient temperature.

*Master equations for quantum transport.* The tight-binding

Hamiltonian for an interacting  $N$ -body system is given by [1]

$$H_S = \sum_{m=1}^N \epsilon_m a_m^\dagger a_m + \sum_{n < m} V_{mn} (a_m^\dagger a_n + a_n^\dagger a_m). \quad (1)$$

This Hamiltonian applies to a large class of quantum transport systems such as excitons and charges in molecular crystals and quantum dots [21, 22]. The  $a_m^\dagger$  and  $a_m$  are the creation and annihilation operators for an excitation at site  $m$ , leading to the singly-excited states  $|m\rangle = a_m^\dagger |0\rangle$ , where  $|0\rangle$  is the system ground state. For the decoherence model used in this work the creation and annihilation operators only need to satisfy the property  $a_m^\dagger a_n |n'\rangle = \delta_{nn'} |m\rangle$  [8]. The site energies and two-body interactions are given by  $\epsilon_m$  and  $V_{mn}$  respectively. The site energies, or static disorder, can be due to different local environments of otherwise identical molecules or due to fabrication imperfections of engineered structures. For chromophores, the coupling is mediated by the Coulomb interaction (Förster coupling) or electron exchange (Dexter coupling). It is appropriate to study the dynamics only in the *single exciton manifold*, spanned by the states  $|m\rangle$ . This is because  $H_S$  preserves the number of excitations and also because exciton recombination has a characteristic time scale of 1 ns, [24], much longer than the usual time scales of the Hamiltonian (1) [15, 25, 26]. Finally, coherences between ground and excited states, such as  $|0\rangle\langle m|$ , have an estimated decay time of about 5 fs [6], and thus can be safely neglected.

A multichromophoric system interacts with the surrounding environment, such as the solvent or the protein, which is usually a macroscopic system with many degrees of freedom. Thermal fluctuations of the environment couple to the chromophores by the electron-phonon Hamiltonian

$$H_{SB}(t) = \sum_{m,n} q_{mn}(t) a_m^\dagger a_n, \quad (2)$$

where  $q_{mn}(t)$  describes the bath fluctuations in the interaction picture. The overall Hamiltonian  $H_S + H_{SB}$  preserves the number of excitations. Yet the coupling to the phonon bath,  $q_{mn}(t) a_m^\dagger a_n$ , leads to irreversible dynamics characterized by relaxation of an exciton from a high- to a low-energy state and dephasing of exciton coherences. Depending on the temperature, the energy relaxation of an exciton occurs on a time scale of  $\sim 1$  ps, while dephasing occurs on a time scale of 100 fs [9].

To a certain approximation, the decoherence part of the equation of motion for a multi-level system in the presence of Markovian fluctuations is dominated by pure dephasing of exciton coherences [8, 9]. This is especially the case at high temperatures. The Liouville-von Neumann equation for the system and bath density operator is  $\dot{\rho}_{\text{tot}}(t) = -\frac{i}{\hbar} [H_S + H_{SB}(t), \rho_{\text{tot}}(t)]$ . Averaging over the phonon degrees of freedom one obtains an effective master equation for the system density operator,  $\dot{\rho}(t) = -\frac{i}{\hbar} \langle [H_S + H_{SB}(t), \rho_{\text{tot}}(t)] \rangle_B$ . The bath operators  $q_{mn}(t)$  are taken to be unbiased Gaussian fluctuations, with  $\langle q_{mn}(t) \rangle_B = 0$  and a two-point correlation function

$$\langle q_{kl}(t) q_{mn}(0) \rangle_B = \delta_{kl} \delta_{lm} \delta_{mn} \delta(t) \gamma_m, \quad (3)$$

where  $\gamma_m$  is a site-dependent rate. Eq. (3) implies the following assumptions [9, 21, 26]: First, only diagonal fluctuations are considered, a reasonable approximation for most chromophores where the molecular transition frequency is much larger than the inter-molecular coupling. Second, we assume that fluctuations at different sites are uncorrelated. Finally, we assume that the phonon correlation time is small compared to the system timescales, an assumption that is justified at room temperatures where the phonon correlation time is estimated to be below 50 fs [9]. Additionally, the correlator is assumed to be site-independent,  $\langle q_{mm}(t) q_{mm}(0) \rangle_B = \gamma_\phi \delta(t)$ , so all chromophores experience the same coupling strength to the environment,  $\gamma_\phi$ . With these assumptions, one obtains the Haken-Strobl equation for the density operator in the Schrödinger picture as [8]

$$\dot{\rho}(t) = -\frac{i}{\hbar} [H_S, \rho(t)] + L_\phi(\rho(t)), \quad (4)$$

where the pure-dephasing Lindblad operator is given by

$$L_\phi(\rho(t)) = \gamma_\phi \sum_m [A_m \rho(t) A_m^\dagger - \frac{1}{2} A_m A_m^\dagger \rho(t) - \frac{1}{2} \rho(t) A_m A_m^\dagger]. \quad (5)$$

with the generators  $A_m = |m\rangle\langle m|$  and a pure dephasing rate is given by  $\gamma_\phi$ . This Lindblad equation leads to exponential decay of all coherences in the density operator.

*Energy transfer efficiency and transport time.* There are many possible ways to measure or quantify the success rate of an energy transfer process, such as energy transfer efficiency and transfer time [23, 25, 27, 28, 29]. First, in order to account for exciton recombination and exciton trapping, we augment the Hamiltonian (1) with an anti-Hermitian part [15, 30],

$$H_{\text{diss}} = -i\hbar\Gamma \sum_m a_m^\dagger a_m - i\hbar \sum_m \kappa_m a_m^\dagger a_m. \quad (6)$$

The excitation is dissipated with a rate  $\Gamma$  at every site and trapped with a rate  $\kappa_m$  at certain molecules [7, 9, 23, 27, 31]. The probability that the exciton is successfully captured at a target site  $m$  within the time interval  $[t, t + dt]$  is given by  $2\kappa_m \langle m | \rho(t) | m \rangle dt$ . Thus, the efficiency can be defined as the integrated probability of trapping at multiple sites as:

$$\eta = 2 \sum_m \kappa_m \int_0^\infty dt \langle m | \rho(t) | m \rangle. \quad (7)$$

In general, the efficiency differs from unity due to finite exciton lifetimes ( $\sim 1$  ns). Another relevant measure for a quantum transport process is the average transfer time defined as

$$\tau = \frac{2}{\eta} \sum_m \kappa_m \int_0^\infty dt t \langle m | \rho(t) | m \rangle. \quad (8)$$

The use of the efficiency as a means of describing transport has considerable benefits over approaches that only consider the limiting distribution [13]. The limiting distribution of a pure-dephasing master equation, such as Eq. (4), is an equal population of all sites, which is the same as for a classical random walk on a regular graph [13]. The limiting distribution

does not take into account the physically relevant short-time behavior where quantum evolution dominates.

*Environment-assisted quantum transport (ENAQT).* The efficiency of quantum transport in an open system can be substantially enhanced by the interaction with a fluctuating environment. The master equation (4) is a specific example of a large class of transport master equations representing site-to-site hopping situations. As noted above, the Hamiltonian part of these master equations has a diagonal part representing the energies of the individual sites, while the off-diagonal part represents hopping terms. The open-system Lindblad operators in the master equation are dominated by terms that dephase the system in the site basis. Relaxation, another possible non-unitary contribution to the quantum transport involving energy exchange with the environment, is slow compared with dephasing. The dephasing rate is slow at low temperatures, and fast at high temperatures. Based on fundamental physical principles, we can make the following set of phenomenological predictions for such decohered quantum evolution. As will be seen, these predictions are borne out in detail by the simulated behavior of the Fenna-Matthews-Olson complex and in binary trees. We predict that the same generic behavior will hold for decohered quantum walks in general.

At low temperatures, the dynamics is dominated by coherent hopping. Because of the variation in the energy levels of different sites and in the strength of the hopping terms, the system is disordered and exhibits Anderson localization [10]. The degree of localization depends on the variation in the energies: for small variation, the system should exhibit weak localization, and for large variation, strong localization should take place. Note that the characteristic behavior of Anderson localization can occur even in a system with only a few sites [32]. In this case, localization can be thought of in terms of energy conservation: an excitonic state originally localized at an initial site is a superposition of energy eigenstates that exhibits only a slight overlap with an excitonic state localized at a final state with significantly different site energy. As a result, coherent hopping on its own has a low efficiency for transporting an excitation from one site to another with significantly different site energy.

As the temperature rises, dephasing comes into play. At first, it might seem that dephasing in the site basis can have no role in enhancing transport, as this form of noise induces no transport on its own. A moment's reflection, however, reveals that this expectation is incorrect. Localization is caused by coherent interference between paths; if that coherence is destroyed, then the localization effect is mitigated. Coherence causes an excitation to become 'stuck.' It might oscillate back and forth between a few sites that are strongly coupled and have similar energies, but the exciton will never venture far afield. By destroying the coherence of the beating, dephasing also destroys the localization and allows the exciton to propagate through the system. This phenomenon, by which decoherence enhances transport, affects all such hopping systems.

When the dephasing rate grows larger than the terms of the system Hamiltonian we expect transport to be suppressed again. This suppression of transport by high dephasing can be thought of as an example of the watchdog (quantum Zeno)

effect [20, 33, 34]: rapid dephasing at a rate  $\gamma_\phi$  in the site basis is equivalent, so far as the system is concerned, to being measured repeatedly in the site basis at time intervals  $\approx \gamma_\phi^{-1}$ . The watchdog effect will then suppress transport away from the initial site. While these predictions hold for a large class of transport systems, we study these effects for a two-chromophore system, the Fenna-Matthews-Olson complex and binary-tree structures.

*Quantum transport in a two chromophore system.* A particularly simple and illustrative example is to study quantum transport in a system of two sites: a particle hops from site 1 to 2 with a significant energy mismatch between 1 and 2. With  $|1\rangle$  and  $|2\rangle$ , the states where the exciton is localized at site 1 and 2, respectively, the Hamiltonian for such a system can be written  $H = \epsilon/2(|1\rangle\langle 1| - |2\rangle\langle 2|) + V/2(|1\rangle\langle 2| + |2\rangle\langle 1|)$ , where  $\epsilon$  is the energy mismatch between 1 and 2, and  $V$  is the strength of the hopping term. As usual, we define the Larmor frequency  $\hbar\Omega = \sqrt{\epsilon^2 + V^2}$ . The coherent evolution of the system, starting from site 1, is simply a rotation about an axis displaced by an angle  $\theta = \sin^{-1}(V/\hbar\Omega)$  from the  $z$ -axis in the  $x - z$  plane. The maximum probability of finding the system at site 2 is  $\sin^2 2\theta$ , and the average probability of finding it there is  $\sin^2 \theta$ . If the energy mismatch is sufficiently large, substantial hopping does not occur and the system remains localized at site 1.

In the presence of decoherence, the system obeys the Bloch equation. Pure dephasing corresponds to a Lindblad operator  $\sqrt{\gamma_\phi}(|1\rangle\langle 1| - |2\rangle\langle 2|)$ , where  $\gamma_\phi = 1/T_\phi$ . The conventional Bloch analysis now holds. When  $\gamma_\phi$  is of the same order as  $\Omega$ , the system, instead of remaining localized at site 1, gradually diffuses, ultimately becoming a uniform mixture of  $|1\rangle$  and  $|2\rangle$ . In the equilibrium state the system has a 50% chance of being found at site 2. The diffusion process can be thought of as a random walk on the Bloch sphere with step length  $\theta$  and with time per step  $\gamma_\phi^{-1}$ . Accordingly, the system must perform  $\approx (\pi/\theta)^2$  steps and the diffusion time is  $\tau_{\text{diff}} \approx (\pi/\theta)^2 \gamma_\phi^{-1}$  to reach a steady state. For a system with more than two sites, the transport will be more complicated. Nevertheless, we still expect the transport rate to increase in direct proportion to the inverse of the individual site decoherence time. This is indeed true if the decoherence time does not substantially exceed the time scales defined by the transport terms in the Hamiltonian and the energy mismatch from site to site. This fact supports the second prediction of environmentally assisted quantum transport.

In the case of rapid dephasing,  $\gamma_\phi > \Omega$ , the angle  $\phi$  that the system precesses before being decohered is  $\approx \Omega/\gamma_\phi$ . The probability of remaining in site 1 becomes  $\cos^2 \phi \approx 1 - (\Omega/\gamma_\phi)^2$ . The system essentially performs a biased random walk with step size  $\phi$  and an average time per step of  $(\gamma_\phi/\Omega)^2 \gamma_\phi^{-1} = \gamma_\phi/\Omega^2$ . In time  $t$ , the system diffuses by an angle  $\Omega\sqrt{t/\gamma_\phi} \cdot \Omega/\gamma_\phi = \Omega^2 t^{1/2} \gamma_\phi^{-3/2}$ . In the case that the system has more than two states, we still expect this analysis to hold, taking  $\gamma_\phi$  to be the dephasing rate and  $\Omega$  to be an average eigenfrequency. This supports our third prediction: as the dephasing rate grows larger than the Hamiltonian energy scale, the transport rate is suppressed by a polynomial in the dephasing rate. These general properties of ENAQT are also

observed by the detailed simulations of the FMO complex and binary tree structures.

*Quantum transport in Fenna-Matthews-Olson protein complex.* The Fenna-Matthews-Olson protein of the green sulphur bacterium *Chlorobium tepidum* [2, 21, 35] is a trimer in which each of the three subunits has seven chlorophyll molecules spatially arranged within a distance of several nm [36]. The FMO complex transfers excitation energy from the chlorosomes, the main light-harvesting antennae, to a reaction center where a charge separation event and subsequent biochemical reactions occur. In analogy to the two-level system discussed above, we expect the same environment-assisted dynamical behavior in the FMO complex monomers. The dynamics are governed by a Hamiltonian of the form Eq. (1) for seven sites with a distribution of site energies and inter-site couplings as given in Ref. [21]. The chromophoric Förster couplings are on the order of  $200 \text{ cm}^{-1}$ . The chlorophyll transition frequencies are shifted by the electrostatic protein environment, resulting in site-dependent electrochromic shifts of up to  $300 \text{ cm}^{-1}$  [26, 35]. Fluctuations of the protein in the solvent lead to fluctuations of the transition frequency of the chlorophylls and therefore to loss of excitonic phase coherence. To describe this effect, we use the master Eq. (4) with a site-independent dephasing rate  $\gamma_\phi$  according to the Haken-Strobl model. This approach is not the standard method for describing decoherence effects within the FMO complex [15, 21]. However, the Haken-Strobl model has been used to describe the quantum dynamics of chromophoric arrays [7, 9] and is expected to deliver insight into the high temperature behavior of the FMO protein.

The initial state for our simulation of the system is a statistical mixture of localized excitations at sites 1 and 6, the chlorophyll molecules that are close to the chlorosome antenna. In the FMO complex, chromophore 3 is in the vicinity of the reaction center [26, 35, 36]. Thus, one can assume that chlorophyll 3 is the main excitation donor to the reaction center [15]. The precise transfer rate to the reaction center is not fully characterized. Yet, based on typical transfer rates in chromophoric complexes with similar inter-molecular distances, we estimate it to be  $\kappa_3 = 1 \text{ ps}^{-1}$  [15]. Thus, the efficiency of energy transfer according to Eq. (7) becomes  $\eta = 2\kappa_3 \int_0^\infty dt \langle 3|\rho(t)|3 \rangle$ .

In Fig. 2 (upper panel) the efficiency of transfer and the transfer time is given as a function of the dephasing rate  $\gamma_\phi$ . At low dephasing purely quantum mechanical evolution leads to an efficiency of around 80%. The excitation stays largely localized at site 1 or 6, having only a small overlap with target site 3. With increasing dephasing the efficiency increases considerably, up to 94%, where it approximately remains constant for a range of  $\gamma_\phi$  of one order of magnitude. For stronger dephasing the efficiency is slowly suppressed again, delocalization is destroyed, and the overlap with the target site vanishes. The transfer time is 75 ps in the fully quantum limit and improves significantly to 7 ps in the intermediate ENAQT regime. For large dephasing, the transfer slows down to 500 ps, the same order of magnitude as the excitation lifetime: thus, most of the energy is dissipated to the environment. One can estimate the dephasing rate as a function of temperature with the conventional assumption of an Ohmic

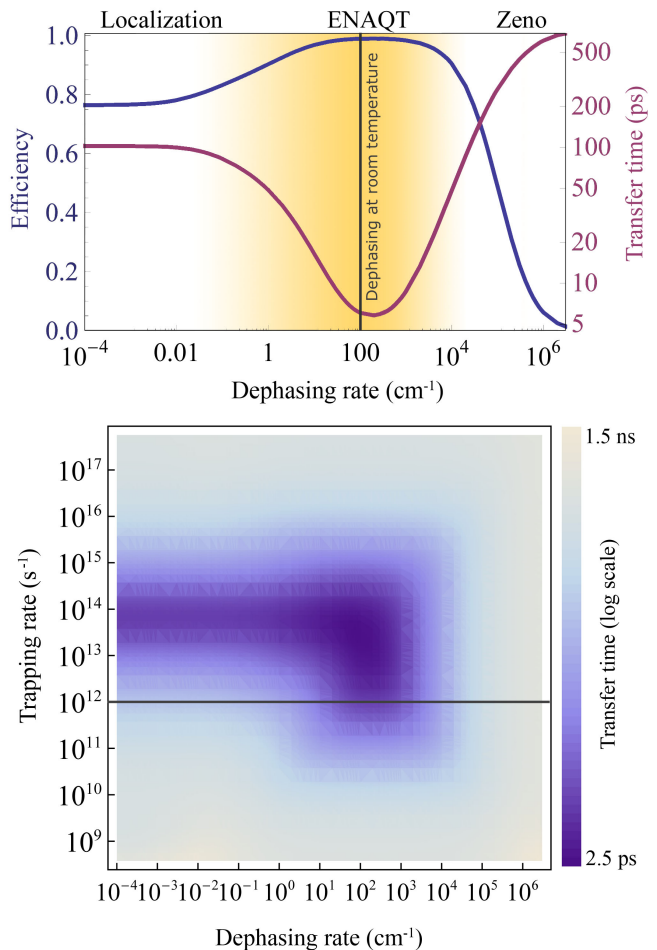


FIG. 2: (Upper panel) Efficiency (blue) and transfer time (red) as a function of the pure-dephasing rate is demonstrated for the Fenna-Matthew-Olsen complex. A clear picture of the three dephasing regimes is obtained: from left to right, the fully quantum regime which is dominated by intrinsic static disorder in the free Hamiltonian; the ENAQT regime (qualitatively indicated by the yellow color gradient), where unitary evolution and dephasing collaborate with the result of increased efficiency; finally, the quantum Zeno regime, where strong dephasing suppresses the quantum transport. As a guide to the eye, the estimated dephasing rate at room temperature for the FMO spectral density (see text) is drawn. The trapping rate is  $\kappa_3 = 1 \text{ ps}^{-1}$ . (Lower panel) Transfer time as a function of dephasing rate and trapping rate  $\kappa_3$  is illustrated on a log scale. The upper panel is indicated as a horizontal line.

spectral density with cutoff,  $J(\omega) = \frac{E_R}{\hbar\omega_c} \omega \exp(-\omega/\omega_c)$ . For the FMO complex, the reorganization energy is found to be  $E_R = 35 \text{ cm}^{-1}$  [21] and the cutoff  $\omega_c = 150 \text{ cm}^{-1}$ , inferred from Fig. 2 in Ref. [26]. The dephasing rate as a function of temperature in the thermal regime  $t \gg \hbar/kT$  is given by  $\gamma_\phi(T) = 2 \frac{kT}{\hbar} \left. \frac{\partial J(\omega)}{\partial \omega} \right|_{\omega=0} = 2 \frac{kT}{\hbar} \frac{E_R}{\hbar\omega_c}$  [6, 37]. This gives a rough estimate for the dephasing rate at room temperature of around  $100 \text{ cm}^{-1}$ , which is indicated in Fig. 2. Hence the natural operating point of the FMO is well within the regime

of ENAQT, where the dephasing introduced by a fluctuating environment enhances the energy transfer efficiency. In Fig. 2 (lower panel), the transfer time is shown as a function of dephasing rate and trapping time  $\kappa_3$ . An optimal region with respect to dephasing rate and trapping rate is discernible. A similar plot was obtained for a model geometry without static disorder and using an effective trapping rate as a measure in Ref. [7].

*Quantum transport in binary tree structures.* Binary trees appear in a wide variety of situations, ranging from computer science [38] to quantum physics and quantum information science [13]. Specifically, they arise in classical and quantum random walks [13] and certain molecular structures such as dendrimers [39]. The effect of static disorder of the energy levels in quantum walks on binary trees has been studied in Refs. [12, 28] where it was argued that such disorder diminishes the exponential speed-up in finding particular target sites, a consequence of Anderson localization. The presence of disorder could restrict the applicability of binary tree structures for devising quantum algorithms or for transporting quantum particles. In this section, we demonstrate that ENAQT also occurs in a statically disordered binary tree structure leading to a substantial improvement in quantum transport.

The Hamiltonian of a disordered graph of generation  $g$  is

$$H_S = \sum_{m=1}^{2^g-1} \epsilon_m |m\rangle\langle m| \quad (9)$$

$$+ V \sum_{m=1}^{2^{g-1}-1} (|m\rangle\langle 2m| + |m\rangle\langle 2m+1| + \text{h.c.}).$$

The site energies  $\epsilon_m$  are taken to be normally distributed about a common value  $\epsilon_0$ , where the standard deviation of the distribution,  $\delta$ , is the characteristic parameter of the static disorder. The hopping strength  $V$  is uniform over the full graph and connects the sites as depicted in Fig. 1b. In the case of static disorder, the full Hilbert space has to be taken into account and consequently a reduction to a quantum walk on the line, as in [12, 13], is not possible. Additionally, we introduce an excitation loss rate  $\Gamma$  and an excitation trapping rate  $\kappa$ , leading to the non-Hermitian Hamiltonian  $H_{\text{diss}} = -i\hbar\Gamma \sum_{m=1}^{2^g-1} |m\rangle\langle m| - i\hbar\kappa|1\rangle\langle 1|$ , where 1 is the root of the tree. This defines the efficiency of transfer, Eq. (7). For the time evolution, we assume an initial state where all the sites in the outermost branch are populated in a classical mixture or a coherent superposition.

Fig. 3 shows the dependence of the efficiency on the characteristic disorder parameter  $\delta$  for a fourth-generation binary tree (15 sites) using the parameters  $\Gamma = 0.005V$  and  $\kappa = 2V$ . The purely quantum case is compared to the case where the

introduction of dephasing leads to an optimal enhancement of the energy transfer efficiency. For the initial state which is a coherent superposition of all sites in the outermost branch, one can clearly see that static disorder leads to a reduced transport efficiency. The broadening around the mean in the plot is due to the random distribution of the site energies over the whole graph. The efficiency decrease is readily explained by localization, see discussion above and Ref. [12]. In the ENAQT regime, with pure dephasing taken to be uniform over the whole graph, one obtains the maximal improvement in transfer efficiency, given by the orange line in the graph. The average maximal improvement is higher the more static disorder is in the system.

The picture becomes more involved when a classical mixture of excitations in the outermost branch is taken as an initial state. Since the initial state is not a column eigenstate that preserves the symmetry of the graph, the purely quantum case without static disorder shows only small transport efficiencies of 20%. Additional static disorder on average increases the efficiency to a maximum of 60% when  $\delta/V \approx 1$ . Here, static disorder creates higher localization at the root of the tree at site 1. For larger static disorder one obtains the same suppression of the efficiency as for the coherent initial state. In the presence of environmental fluctuations one obtains an overall average improvement for all static disorder regimes: for small static disorder the improvement is 60%, for intermediate it is 20%, and for larger disorder it is around 40%. In summary, ENAQT is shown to consistently improve the transport efficiency in binary tree structures, overcoming localization induced by the initial state of the system and static disorder.

*Conclusion.* Environmentally assisted quantum transport is a fundamental effect which occurs in a wide variety of transport systems. ENAQT is similar in flavor to stochastic resonance [17]: adding noise to a coherent system enhances a suitable transition rate. ENAQT differs from stochastic resonance in that the system whose transition rate is enhanced is undriven and does not need to be in some strong nonlinear regime. The maximum efficiency of ENAQT occurs when the decoherence rate is comparable to the energy scales of the coherent system as defined by the energy mismatch between states and the hopping terms. By changing the energy mismatch and the hopping terms, one can tune the temperature at which the maximum transport efficiency occurs. In the Fenna-Matthews-Olson protein complex and with the spectral density as discussed above, this maximum occurs at approximately room temperature, suggesting that quantum transport optimization via natural selection may have taken place.

We would like to acknowledge useful discussions with G.R. Fleming and C.A. Rodriguez-Rosario. We thank the Faculty of Arts and Sciences of Harvard University, the Army Research Office (project W911NF-07-1-0304), and Harvard's Initiative for Quantum Science and Engineering for funding.

[1] V. May and O. Kuhn, *Charge and Energy Transfer Dynamics in Molecular Systems* (Wiley-VCH, Weinheim, 2004).

[2] G.S. Engel, T.R. Calhoun, E.L. Read, T.-K. Ahn, T. Mancal, Y.-C. Cheng, R.E. Blankenship, and G.R. Fleming, *Nature* **446**,

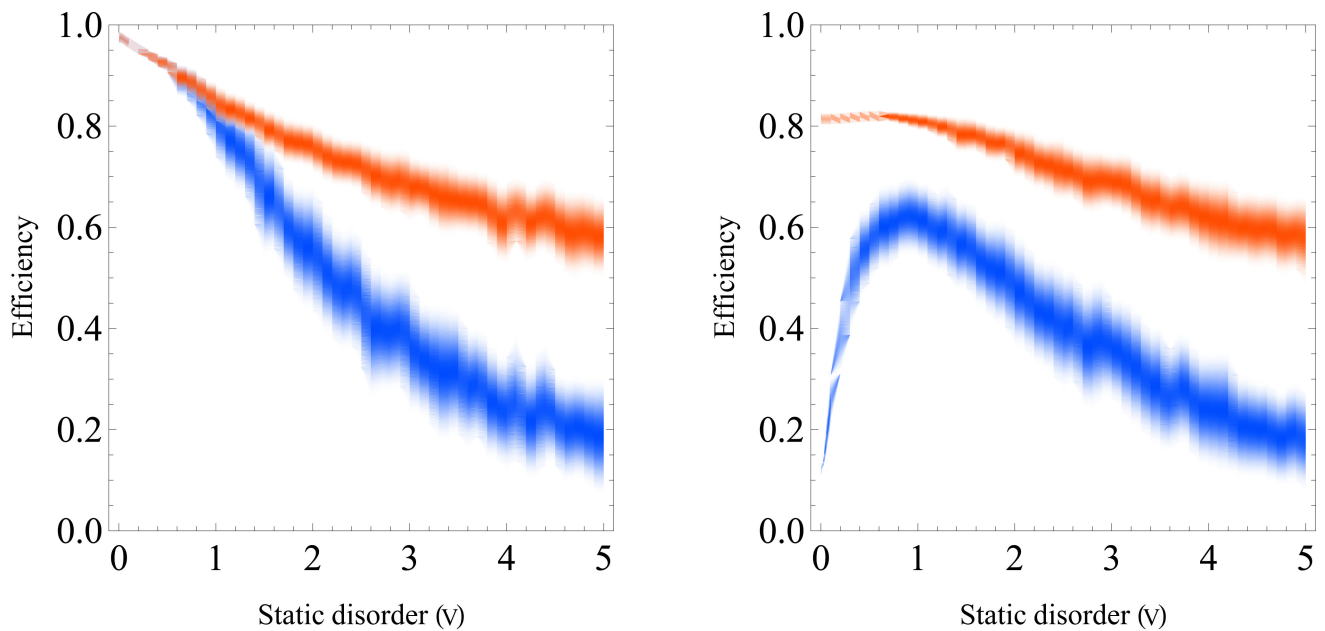


FIG. 3: The variation of efficiency as a function of the static disorder parameter  $\delta$  for a four-generation binary tree. A coherent superposition (left panel) or a statistical mixture (right panel) of the outermost branch of the tree was chosen as an initial state (cf. Fig. 1b, grey sites). Optimal ENAQT (orange) shows a considerable improvement over the fully quantum case (blue). 100 randomly sampled graphs were used per data point, leading to a distribution of efficiencies. Parameters are  $\Gamma = 0.005V$  and  $\kappa = 2V$ .

- 782 (2007).
- [3] H. Lee, Y.-C. Cheng, and G.R. Fleming, *Science* **316**, 1462 (2007).
- [4] M. Grover, R. Silbey, *J. Chem. Phys.* **54**, 4843 (1971).
- [5] M. Yang, G.R. Fleming, *Chem. Phys.* **275**, 355 (2002).
- [6] J. Gilmore, R.H. McKenzie, *J. Phys. Chem. A*, **112**, 2162 (2008).
- [7] K.M. Gaab, C.J. Bardeen, *J. Chem. Phys.* **121**, 7813 (2004).
- [8] H. Haken, G. Strobl, *Z. Physik* **262**, 35 (1973).
- [9] J.A. Leegwater, *J. Phys. Chem.* **100**, 14403 (1996).
- [10] P.W. Anderson, *Phys. Rev.* **109**, 1492 (1958).
- [11] P.W. Anderson, *Rev. Mod. Phys.* **50**, 191 (1978).
- [12] J.P. Keating, N. Linden, C.F. Matthews, A. Winter, *Phys. Rev. A* **76**, 012315 (2007).
- [13] A. Childs, E. Farhi, and S. Gutmann, *Quant. Info. Proc.* **1**, 35 (2002).
- [14] E. Rozbicki, P. Machnikowski, *Phys. Rev. Lett.* **100**, 027401 (2008).
- [15] M. Mohseni, P. Rebentrost, S. Lloyd, A. Aspuru-Guzik, arXiv:0805.2741 (2008).
- [16] P. Rebentrost, M. Mohseni, A. Aspuru-Guzik, arXiv:0806.4725 (2008).
- [17] L. Gammaitoni, P. Hänggi, P. Jung, F. Marchesoni, *Rev. Mod. Phys.* **70**, 223 - 287 (1998).
- [18] P. E. Parris and P. Phillips, *J. Chem. Phys.* **88**, 3561 (1988).
- [19] P. Phillips, *Annu. Rev. Phys. Chem.* **44**, 115 (1993).
- [20] B. Misra, E. C. G. Sudarshan, *J. Math. Phys.* **18**, 756 (1977).
- [21] M. Cho, et al., *J. Phys. Chem. B* **109**, 10542 (2005).
- [22] A. Nazir, B.W. Lovett, S.D. Barrett, J.H. Reina, and G.A.D. Briggs, *Phys. Rev. B* **71**, 045334 (2005).
- [23] M.K. Sener, D. Lu, T. Ritz, S. Park, P. Fromme, and K. Schulten, *J. Phys. Chem. B* **106**, 7948 (2002).
- [24] T.G. Owens, S.P. Webb, L. Mets, R.S. Alberte, and G.R. Fleming, *Proc. Natl. Acad. Sci. USA* **84**, 1532 (1987).
- [25] T. Ritz, S. Park, and K. Schulten, *J. Phys. Chem. B* **105**, 8259 (2001).
- [26] J. Adolphs, T. Renger, *Biophys. J.* **91**, 2778 (2006).
- [27] M.K. Sener, S. Park, D. Lu, A. Damjanović, T. Ritz, P. Fromme, and K. Schulten, *J. Chem. Phys.* **120**, 11183 (2004).
- [28] O. Muelken, V. Bierbaum, A. Blumen, *J. Chem. Phys.* **124**, 124905 (2006).
- [29] A. Olaya-Castro, C. Fan Lee, F. Fassiolli Olsen, and N. F. Johnson, arXiv:0708.0436 (2007).
- [30] S. Mukamel, *Principles of Nonlinear Optical Spectroscopy*, Oxford University Press, New York (1995).
- [31] O. Mülken, A. Blumen, T. Amthor, C. Giese, M. Reetz-Lamour, and Matthias Weidemüller, *Phys. Rev. Lett.* **99**, 090601 (2007).
- [32] M.K. Henry, J. Emerson, R. Martinez, D.G. Cory, *Physical Review A* **74**, 062317 (2006).
- [33] N. Erez, G. Gordon, M. Nest, G. Kurizki, *Nature* **452**, 724 (2008).
- [34] A. G. Kofman and G. Kurizki, *Nature* **405**, 546 (2000).
- [35] F. Müh, M. El-Amine Madjet, J. Adolphs, A. Abdurahman, B. Rabenstein, H. Ishikita, E.-W. Knapp, and T. Renger, *Proc. Natl. Acad. Sci. USA* **104**, 16862 (2007).
- [36] Y. Li, W. Zhou, R. E. Blankenship, and J. P. Allen, *J. Mol. Biol.* **271**, 456 (1997).
- [37] H. -P. Breuer and F. Petruccione, *The Theory of Open Quantum Systems* (Oxford University Press, New York, 2002).
- [38] D. Knuth. *The Art of Computer Programming*, Vol 1-3, Addison-Wesley (1997).
- [39] Z. He, T. Ishizuka, and D. L. Jiang, *Polymer J.* **39**, 889 (2007).